

Analysis on the Rail Gnawing Force of Bridge Cranes

—A Study Based on Finite Element Technology

Yefeng Jiang

Jiaying Institute of Special Equipment Inspection, China

Keywords: rail gnawing, bridge cranes, finite element technology.

Abstract: Rail gnawing means that, when the bridge crane is in operation, the wheel flanges of traveling mechanism and trolleys contact with track side and causes level lateral thrust, leads to the friction and wear of tracks and wheel flanges. The phenomenon of rail gnawing is inevitable after the running of crane for a period of time; serious rail gnawing can lead to severe wear of tracks and wheels, as well as equipment accidents. Therefore, it is necessary to analyze the rail gnawing phenomenon caused by cranes, then find problems in time and improve relevant solutions, in order to effectively reduce the failure rate of equipment and reduce the downtime of lifting machinery.

1. Introduction

During the operation of cranes, the running of travelling mechanism can cause serious rail gnawing and the severe wear of tracks and wheels, which will greatly increase the additional load and running resistance, and cause the torsional pendulum of cranes. The transmission mechanism and running motor will be overload; equipment accidents like broken transmission shaft and burnt motor may appear and increase the wear of components and maintenance costs. More serious consequences even include derailment accidents, which can cause great security risks and seriously affect the production process. In enterprise production, cranes play an extremely important role; the working conditions of cranes directly affect the production process. Therefore, it is necessary to analyze the rail gnawing phenomenon caused by cranes.

2. Analysis on Reasons of Rail Gnawing

Bridge cranes produce longitudinal and lateral forces when they are in operation. If the traveling mechanism and trolleys are braked simultaneously, the braking force will be produced; the track need to bear slant tension. When there is a height difference between the two sides of the track, all the gravity of the crane will move to the lower side, increasing the lateral force suffered by the track. The wheels on one side of the track are tightly clamped to the outer side of the track, causing the gnawing of rails. A little bit of rail gnawing can cause significant wear marks on the side of wheel rims and tracks; serious rail gnawing can cause side metal stripping of tracks and the outward deformation of wheel rims. There are various reasons of rail gnawing, which need to be analyzed in detail. The main causes can be divided into following categories: tracks (parallelism, height difference, gauge, horizontal bending and pressing plate), wheels (wheel diameter, roundness, height difference, horizontal bending and vertical bending), crane span structure (vertical deformation of the main beam, horizontal bending of main beam, vertical bending of the end beam and horizontal bending of the end beam) and other factors (different speed of electromotor, gaps between couplings and brakes, sundries on the end face of track).

The working environments of cranes are different, which lead to diversified rail gnawing phenomena. Rail gnawing caused by bridge cranes can produce cracks on the surface of wheels and affect the performances of wheels. It can also lead to the abrasion of flange thickness, the bending and deformation of rims, and the wear of treads. The problem of lose efficacy comes afterwards. Finding out the causes and corresponding reasons can not only prevent the re-occurrence of failure, but also

improve the functions of crane components, and promote the improvement of related works.

3. The Stress Tests and Results

All instruments and equipments are connected according to the proportional relationship between the mechanical strain and the change of resistance. The empty trolley is stopped at the opposite end of driver's room; all stress channels are adjusted to zero and calibrated. Then the crane is operated according to predetermined requirements; the dynamic strain meter records signals during the whole course.

In the test, the upper cover plate of the north main beam in mid-span and the load dividing dolly of the east end beam are selected as test parts. Since these parts are in the state of unidirectional stress, the single strain gage is used. The layout of test points is shown in Figure 1.

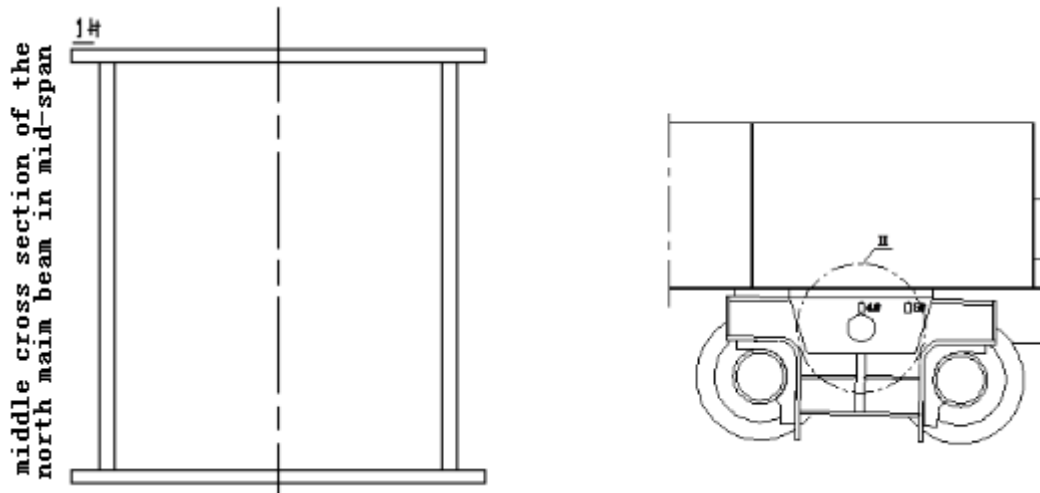


Figure 1. Layout of stress measuring points

The process of the first test goes as following. (1) The travelling mechanism stays still; the empty trolley stops in the East; all instrument are set as zero. (2) Unhook the trolley in the east; the travelling mechanism moves northward while the trolley moves westward; the travelling mechanism adjusts its position. (3) The load hook lifts the weight, falls and releases. (4) The load hook rises, brakes, falls, brakes, rises, brakes, falls, brakes. (5) The travelling mechanism, trolley and load hook are stationary; the static stiffness is measured. The first test aims to evaluate the stress level of the middle cross section of the main beam during the loading process, so only the frequency spectrums of several rising, falling and braking movements and the signal waveform diagram of the 1# strain gage are shown in Figure 2.

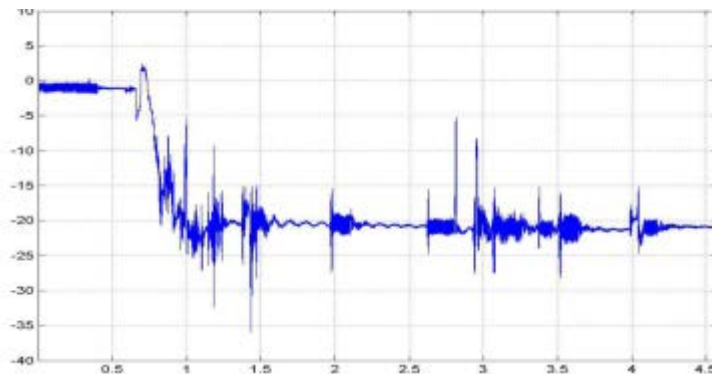


Figure 2. Waveform diagram of stress signals in the mid-span of north main beam

4. Finite Element Modeling Analyses

In this paper, a certain type of bridge crane is studied. Its rated load weight is 30t; the self weight of

trolley is 75t. In the finite element analysis of structures, it is necessary to define the properties of the material: density, Poisson's ratio and elastic modulus. The material studied in this paper is Q235, with Poisson's ratio = 0.33, elastic modulus $E = 210 \text{ GPa}$, density = 7.85 g/cm^3 and tensile strength = 500 MPa . The calculation objects are the overall span structure and the load dividing dolly of the bridge crane. The crane span structure is a box structure. NASTRAN shell elements are used in modeling the webs, upper and lower cover plates of the main and end beams, rib plates and dummy plates in the middle, as well as the rib plates, upper and lower cover plates of the load dividing dolly. Due to the symmetry of this structure, the finite element analysis is carried out for the overall crane span structure and the load dividing dolly. Constraints are added to the wheel tread of load dividing dolly. The eight wheels are divided into four groups. Four groups of wheels can be regarded as the hinge supports; one group is used as the fixed hinge support; the other three groups are used as movable hinge supports. The finite element model of the crane span structure is restrained.

4.1 Calculating load and working condition.

The load is calculated as following:

Live load is presupposed according to the elevating capacity at the measured working condition: $Q=16.8\text{t}$; rated load weight $Q_e=30\text{t}$; weight of the trolley $G_{xc}=75\text{t}$; maximum rake thrust $F_{pmax}=(G_{xc}+Q) \cdot \mu$; lateral rail gnawing force F_l : these elements are linearly distributed to the same side of the dolly wheel. 2) Fixed load: self weight of the main beam: NASTRAN automatic calculation; self weight of the end beam: NASTRAN automatic calculation; self weight of dolly: NASTRAN automatic calculation. 3) Rising impact coefficient: $\Phi_1=1.06$; lifting load dynamic loading coefficient: $\Phi_2=1.1$.

The calculation of load condition 1: the structural stress caused by the maximum rake thrust of the trolley is considered when live load $P = G_{xc}+Q = 75+16.8 = 91.8\text{t}$ is in the mid-span. The value of rail gnawing force is obtained by comparing the calculated result with the measured one.

4.2 Analysis on the calculated result of the stress of middle cross section of the crane span structure in mid-span.

When measured, the trolley is at the eastern end; the instrument is zeroed; the hoisting trolley is lifted and tested for operation. Under the test condition, the full load trolley (lifting test weight $Q=16.8\text{t}$) is in the mid-span. The deformation of the crane span structure is shown in Figure 3 when the maximum rake thrust of the trolley and the maximum 7t gnawing force of the travelling mechanism wheel are considered. The unit of the deformation stress in diagram is MPa.

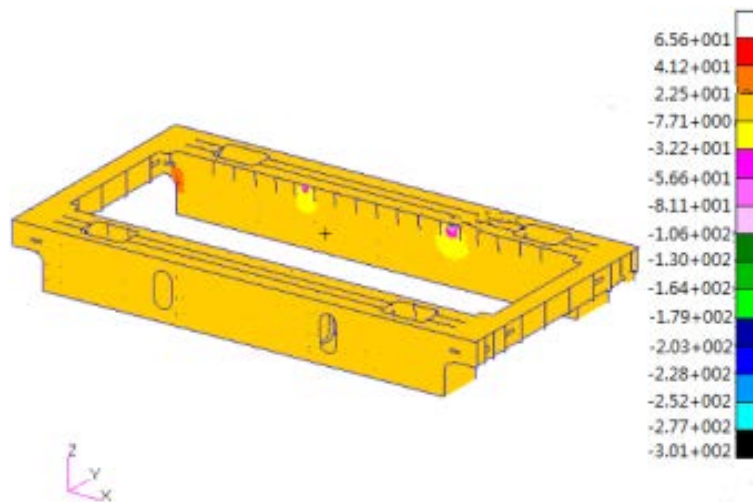


Figure 3. Z direction stress of the crane span structure when the live load is in the mid-span, and the maximum rail gnawing force of travelling mechanism wheel is considered as 7T .

The maximum stress of the middle cross section of the crane span structure occurs when the load trolley is in mid-span. The calculation of finite element analysis corresponds to measured data. The comparison between calculated results and measured values is shown in Table 1.

Table 1 Measured stress and calculated stress of the middle cross section of the crane span structure under test condition 1 Unit: MPa

| measured value | Calculated value | |
|---|----------------------|----------------------|
| middle of the upper cover plate -20.15 | Main beam 1 -21.7 | Main beam 2 -21.2 |

From table 1 it can be seen that the calculated value is very close to measured value under the same working condition, which indicates that the calculation model is correct.

4.3 Analysis on the lateral rail gnawing force of dollies.

During the test, 2 typical test points were selected from one dolly stand. In the finite element calculation, data about the two points are measured when the change of peak stress reach its maximum; a group of data about the maximum and minimum test stress are selected to calculate the mean value. In the process of calculation, the rake stress of the trolley is considered to calculate the lateral rail gnawing force. The finite element analysis of the dolly is shown in Figure 4. In the 2 points, stress amplitude in Z direction of the east end beam dolly in the mid-span has greatest changes; the lateral rail gnawing force at that time is the maximum rail gnawing force that may occur during the operation. The comparisons of the maximum Z direction stress of the east end beam dolly, the maximum 7t lateral gnawing force of the single wheel, the Z direction stress at the corresponding point of dolly stand when the raking force of the trolley is the largest are as follows. The measured maximum value 78.36MPa; the measured minimum value is -58.36MPa; the average amplitude is 68.36MPa; the calculation value in loading condition 1 is 69.23MPa. It can be seen that the average amplitude of the measured value in mid-span of the east end beam dolly is very close to the calculated value. Thus, the maximum lateral gnawing force of the single wheel for the trolley is 7t in the actual operation process.

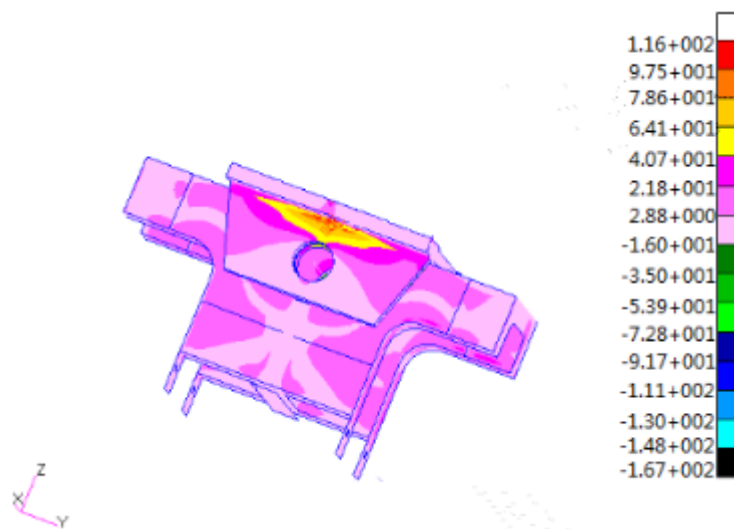


Figure 4. Z direction stress of one dolly when the live load is in the mid-span, and maximum rail gnawing force travelling mechanism wheel is considered as 7t

4.4 Calculation results on stress of crane span structure and dollies and analysis.

The maximum VonMises stress values of the load dividing dolly under different working conditions are shown in Table 2, which removes the stress anomaly in the local area of the loading points.

Table 2 The maximum VonMises stress values of the load dividing dolly under different working conditions unit: MPa

| loading conditions | Description of loading conditions | Maximum VonMises stress of the load dividing dolly |
|--------------------|---|--|
| 2 | Structure stress when live load $P=\Phi 2 (G_{xc}+G)+\Phi 1 Q_e$ is in mid-span | 53.5 |
| 3 | Structure stress when live load $P=\Phi 2 (G_{xc}+G)+\Phi 1 Q_e$ is in end span | 74.5 |
| 4 | Structure stress of dolly caused by the greatest rake force of trolley and the calculated rail gnawing force | 65.6 |
| 5 | Structure stress when live load $P=\Phi 2 (G_{xc}+G)+\Phi 1 Q_e$ is in mid-span, and consider the structure stress caused by the greatest rake force of trolley and the calculated rail gnawing force | 103.3 |
| 6 | Structure stress when live load $P=\Phi 2 (G_{xc}+G)+\Phi 1 Q_e$ is in end span, and consider the structure stress caused by the greatest rake force of trolley and the calculated rail gnawing force | 127.9 |

Comparing above data it can be seen:

(1) Under the condition of 4, the maximum value of the combined stress of the dolly is 65.6MPa, which indicates that the comprehensive stress produced by the structure of dolly under the single lateral force has relatively great influence.

(2) The maximum combined stress of the dolly is 127.9MPa when the maximum lateral rail gnawing force bore by a single wheel of the travelling mechanism is 7t.

(3) The material of the dolly structure is Q235; the strength is checked according to the load combination II; its allowable stress $[\sigma]_{II} = \frac{\sigma_s}{1.33} = 176.7MPa > \sigma_{max} = 127.9MPa$. Thus, the static strength of the crane can meet requirements under the conditions of lateral rail gnawing force and lifting weight.

(4) As far as the fatigue of the structure is concerned, the maximum combined stress of the dolly structure is relatively high with the value of 123.9 MPa. It has relatively great impacts on the fatigue life of the dolly structure.

Through above finite element analysis, it can be seen that the crane's lateral rail gnawing force is larger in running process. Under the influence of rail gnawing force, the static strength of the existing structure of load dividing dolly can basically meet requirements, but has relatively great influences on the fatigue life of the dolly structure.

4.5 Evaluation on lateral rail gnawing force of wheels.

The field measurement shows that the rail gnawing stress is large during the operation of travelling mechanism. For the measured east end beam, in the three test cycles, the maximum stress above the hinged support of dolly in the north is about 80MPa; the minimum stress is about -40MPa. From the measured stress curve, the directions of rail gnawing force of wheels change frequently during the operation of travelling mechanism; the stress range is near 130MPa. And in the simple process of running the travelling mechanism (without other operations), the directions of the stress range of testing points above the hinged support of two dollies at the same end are generally reverse. It is believed that the cause of above phenomenon is the difference between the wear degree of two dollies' wheel flanges, or error in the glancing flatness of four wheels on the same side during installation.

Carefully analyzing the measured stress signals under different operating conditions, it can be found that the measured stress of the load dividing dolly on the same end beam is often the stress at

the same side (in the three test cycles of this paper are positive stress). The four wheels of the same side end beam are basically subjected to gnawing force from the same side. The finite element simulation analysis shows that the rail gnawing force of each wheel is about 7t.

5. Conclusion

Through the finite element analysis and experimental verification, the reasons of rail gnawing can be found effectively and reasonably; countermeasures can be put forward at the same time to guarantee the rationality and effectiveness of the anti-rail gnawing scheme. By means of finite element analysis, the amount of lateral rail gnawing force when the bridge crane is in operation can be determined, which can provide reliable analysis basis for the occurrence of rail gnawing phenomenon and countermeasures.

References

- [1] D.W. Huang, Modern Lifting and Transportation Machinery, Industrial Press, Beijing, 2009.
- [2] L.S. Tang, W.M. Cheng, Design of multi-layer spiral winding transition block, J. Lifting and Transport Machinery. 4 (2011).
- [3] Q. Yu, G.J. Liu, J. Tan, Cause analysis and solution of slugging and gnawing of bridge cranes, J. Mechanical & Electrical Engineering Technology. 01(2013).
- [4] C.H. Lee, K.H. Chang, G.C. Jang, et al., Effect of weld geometry on the fatigue life of non-load-carrying fillet welded cruciform joints, J. Engineering Failure Analysis. 16 (2009).
- [5] K. Saiprasertkit, E. Sasaki, C. Miki, Fatigue crack initiation point of load carrying cruciform joints in low and high cycle fatigue regions, J. International Journal of Fatigue. 59 (2014).
- [6] N. Recho, L.C. Foo, M. Faraldi, et al., Fatigue design of cruciform joints including V-notch effect at the weld toe, J. Procedia Materials Science. 3 (2014).
- [7] K. Saiprasertkit, T. Hanji, C. Miki, Fatigue strength assessment of load-carrying cruciform joints with material mismatching in low-and high-cycle fatigue regions based on the effective notch concept, J. International Journal of Fatigue. 40 (2012).